# PY 402: Design and Analysis of Permanent Magnet Penning Trap for AEGIS Collaboration's Antiproton-beam Studies

**Gerard Lawler**

# Contents

## Special Thanks

I would like to thank my research advisors, Nicola Pacifico and Michael Doser, and my academic adviser David Campbell for guiding and supporting me for the last two semesters. I would like to thank my thesis committee members, Professors Lawrence Sulak, James Miller, and John Butler, for their valuable contributions and the gift of their time. Your discussion, ideas, and feedback have been invaluable. I would also like to thank my fellow undergraduate students, research technicians, collaborators, and the multitude others who contributed to this research. I am very grateful to all of you. And I would like to offer a special thanks to Glenn Thayer of the BU Scientific Instrumentation Facility for our invaluable discussions in terms of machining capabilities. I would especially like to thank my amazing family for the love, support, and constant encouragement I have gotten over the years. In particular, I would like to thank my parents and my sisters. You are the salt of the earth, and I undoubtedly could not have done this without you. Your love, laughter and music have kept me smiling and inspired. You are and always will be my family. Without these contributions and support, this thesis work would have been impossible.

## Abstract

In the year 1928, Paul Dirac, a theoretical physicist, proposed the existence of the positron, an antimatter electron.[15] He did so as a convenience to complete his theory on the unification of quantum mechanics and special relativity, but this turned out to be more than just a convenience. The positron was experimentally verified soon after by Carl Anderson in 1932.[15] Such was the first experimental observation of a new form of matter. Since, then much thought has gone into attempting to explain and understand these mysterious particles. One of the most interesting features is the interesting property that a particle and its antiparticle will they annihilate one another upon collision, thus one of the most enduring questions is how to explain the asymmetrical amount of matter and antimatter in the universe.

The Antiproton Decelerator (AD), is an antiproton storage ring at CERN from which several international collaborative experiments obtain the antiprotons for their experiments. The AEGIS (Antimatter Experiment: Gravity, Interferometry, and Spectrometry) collaboration seeks to measure the weak equivalence principle of antimatter.[8] In previous work, a device was designed for Generating a Reduced-energy Antiproton Beam using Channeling Electrostatics (GRACE). Its purpose is to extract an antiproton beam of tunable mean energy anywhere from 0.1 to 1 keV, from a beam of energies with an upper limit of 5 MeV. An ion trap (Penning trap) was designed to be placed at the end of the beamline in order to trap antiprotons to assess certain properties of the deflected particles.

Typical Penning traps used for antimatter, nuclear spectrometry, or other nuclear research projects require superconducting solenoids to generate the necessary axial magnetic field, on the order of several Tesla. As a resulted, a large amount of additional apparatus is necessitated for cooling purposes. Large cryostats for example lead to the case where a high magnetic field Penning trap is a large and costly device.[12] This is not desirable, so alternatively, a Penning trap design using rare-earth magnets is much more desirable. The magnetic fields are often only 1 or 2 Tesla but are much more versatile.[12] There exist precedence for compact traps with magnetic fields generated by wedges of NdFeB in the 50 to 100 Kelvin range [7] and other work established created axial magnet arrays with epoxy bonded radially-magnetized segments was used to store anions at room temperature.[26] In order to trap the desire low-energy antiprotons from the GRACE beam extractor, an axial Penning trap has been designed which uses an array of ring magnets concentric with the cylindrical electrodes. Of 100000 trials of potentially trapped particles (under 10keV), 19981 were captured for more than 1 second. This corresponds to a simulated $\approx 20\%$ catch rate. Electrodes at 100 to 300 Volts and a magnetic flux density of 1 Tesla from the neodymium magnets were used.

# Chapter 1: Introduction

## Background

Even with our modern understanding of physics, a number of mysteries remain. One place of particular interest is in the study of the nature of the mysterious substance called antimatter. In the year 1928, Paul Dirac, a theoretical physicist, proposed the existence of the positron, an antimatter electron.[1] He did so as a convenience to complete his theory on the unification of quantum mechanics and special relativity, but this turned out to be more than just a convenience. The positron was experimentally verified soon after by Carl Anderson in 1932.[2] Such was the first experimental observation of antimatter. Since, then much thought has gone into attempting to explain and understand these mysterious particles. Matter and antimatter have the interesting property where they annihilate one another, thus one of the most enduring questions is how to explain the asymmetrical amount of matter and antimatter in the universe. At CERN, some of these great questions are being answered.

The Antiproton Decelerator (AD), is an antiproton storage ring from which several international collaborative experiments obtain the antiprotons for their experiments. The AEGIS (Antimatter Experiment: Gravity, Interferometry, and Spectrometry) collaboration is a collaboration seeking to measure the weak equivalence principle of antimatter.[21] In previous work, a device was designed for Generating a Reduced-energy Antiproton Beam using Channeling Electrostatics (GRACE).[4] Its purpose is to extract an antiproton beam of tunable mean energy anywhere from 0.1 to 1 keV, from a beam of energies with an upper limit of 5 MeV. An ion trap (Penning trap) was designed to be placed at the end of the beamline in order to trap antiprotons to assess certain properties of the deflected particles. A study of particle dynamics relating to ion optics and beam physics was undertaken in order to understand the behavior of the particles. The studies helped accurately simulate particles in the trap in order to create an effective design and to ensure that in simulation, a sufficient number of antiprotons were captured and held for an sufficiently long time while avoiding instabilities which may cause a loss of particles.

The trap will used to trap and measure certain properties of the GRACE beam, a task which has the potential to for use in additional antiproton studies. In the grand scheme of the AEgIS collaboration, the studies will aid in the creation of a slow beam of antiprotons (on the order of keV) for the first ever antimatter interferometry, using a Talbot-Lau interferometer.[1] This interferometery using anti-protons will not only be the first interferometry of charged heavy matter and anti-matter, but will also bean important stepping stone on the way to realize the ultimate goal of using interferometry from anti-hydrogen atoms to determine the affect of gravity on antimatter.[1]

The Penning trap itself is a cylindrical open sided Penning trap with an axial magnetic established via a

selection of ring magnets outside of the electrode chamber, it takes advantage of the approximate quadrupole field at the center to confine particles axially and radially with its magnetic fields. The first portion of the thesis will detail the dynamics of the particles within the trap and the effect of their initial conditions on their ability to stay confined. Simulations were performed using C++ code, using IBSimu libraries[]. Design of the trap using the dynamic simulations was then undertaken using the resources of the BU Scientific Instrumentation Facility (SIF). The simulations have showed that the device is capable of trapping $\approx 15\%$ of particles introduced into its chamber given appropriate timing of turning on the first electrode.

## What is antimatter?

In general, antimatter is a type of matter composed of antiparticles, each of which corresponds to a regular particle. Particle-antiparticle pairs, share some properties, such as mass. Other properties such as charge, lepton number, and baryon number are equal in magnitude but differ in a sign. Collisions of the two lead to both particles annihilation into a number of annihilation products, such as photons, neutrinos, and smaller mass particle-antiparticle pairs. We know that the total energy released during an annihilation event is proportional to the total mass of the particle-antiparticle pair with, $c^2$ , as the constant of proportionality.

There currently exist many unsolved questions concerning the nature of antimatter and its place in the universe. Most notably is the apparent asymmetry between antimatter and matter in the observable universe.[17] Indeed, one would expect for the sake of symmetry to observe equal amounts of the two but this is obviously not true since we have yet to annihilate. In order to understand more fully the nature of antimatter, a number of experiments have been formulated to observe and analyse its properties. The baryon asymmetry as it is also called, can be resolved with in the three following ways[15][16]:

1. baryon asymmetry is not actually accurate and their is some antimatter hidden somewhere
2. baryon asymmetry is accurate so there is a mysterious new symmetry breaking mechanism
3. or the standard model of particle physics somehow excludes gravity

We choose to focus on testing the gravitational effects on antimatter in order to answer some of these questions. Despite the fact that the effects of gravity on regular matter has been heavily studied and is well-understood, to date antimatter gravity has not been investigated since the creation of neutral antimatter atoms is a relatively new development.[8] Indeed low energy antihydrogen production from the ATHENA and ATRAP collaborations at CERN has made the possibility of direct antimatter gravity experiments a realizable goal.[16] In terms of the arguments against antigravity, there are many but they are dependent on the particular model being used and are not universally agreed upon so it is still a valid experiment to undertake.[22]

## AEGIS

AEGIS (Antimatter Experiment: Gravity, Interferometry, and Spectroscopy) is a collaboration at CERN which seeks to understand and eventually measure the weak equivalence principle on antihydrogen atoms. Currently, the experiment is in the development phase and working on the development and implementation of the detector, beam extraction, and interferometry systems.

In order to answer questions such as these, a deeper understanding of the behavior of antimatter is necessary. The AEgIS collaboration at CERN intends to answer one of these questions; does gravity affect antimatter in the same way it affects matter. The collaboration unites physicists from all around the world and from a variety of fields in order to eventually measure the sign of the gravitational constant using antimatter hydrogen atoms. The goal is to generate a beam of anti-protons and shoot them through a device known as a deflectometer.[21] Within the deflectometer a series of gratings used to split the beam into parallel rays, in a periodic pattern. The anti-protons will then arrive at a detector, and form the pattern the annihilations. From one can thus measure how much the particles of different velocities move during their horizontal trajectory (and also relative to beams of light), and thus determine the strength of the gravitational force between the Earth and the anti-protons.

The protons come from the Antiproton Deccelerator (AD) at the main CERN site. When they are made, the primary beam of anti-protons are very high energy but are slowed down significantly by the AD. A secondary beam for use in the AEgIS experiment is currently under development. Experimental results were promising however, interferometry has never been done for charged heavy matter, let alone antimatter. As a result, several modifications are warranted, before interferometry is attempted. However, as the beam passes through the deflectometer, many particles annihilate and the angular scattering of the beam increases leading to much lower flux of particles than what is needed. In addition, there is a background from all the photon, pions, and other particles emitted due to the annihilation. Furthermore, the background is higher energy and faster than the anti-protons, so the background will reach the detector before the antimatter, throwing off measurements. The goals are then to reduce these problems and create a degraded beam which can be used for measurement. Before they can be implemented, the beam path and all the devices affecting must be simulated to ensure that they will work properly and give the correct result.

## GRACE

The basic design for the low energy beam deflector/extractor is given by using the following beam-line elements: Einzel lenses to focus the beam, a collimator to narrow the beam, and momentum selector consisting of high voltage electrodes used to reject the annihilation products and accept only the slow anti-protons for detection. The first element is a collimator. This device serves the simple purpose of acting as an annhilation

site for particles with very high transverse energies. For all intents and purposes these antiprotons are as good as gone in our apparatus. They will invariably annihilate on the walls or other matter surfaces, so it is best that they are annhilated as far away from the detector as possible.

The next element is the einzel lens. This is an electrostatic lens consisting of three circularly symmetric conductors which are concentric with the beam direction. The middles is held at a high voltage and the first and last are grounded. This acts to focus the beam with the added benefit of not changing the energy of the particles, due to the symmetry of the geometry. The original proposition only speculated about the use of an einzel lens to focus the beam. High focusing required incredibly high voltages ($\approx 10^5 V$). A more realistic, kiloVolt range, einzel lens is shown as well Thus an arrangement of to einzel lenses was eventually implemented.

The required potential difference needed to curve a charged particle between the two cylindrical is given by

$$qE = \frac{mv^2}{R_0}$$

where E is the electric field strength, v is the velocity of the particle, m is the mass, and q is the charge. Relativistic effects can be ignored since the antiprotons being extracting have low energies. In addition, magnetic effects were ignored because currents were so small. The particles kinetic energies were then said to be classical, such that mv 2. The electric field between the electrodes needed to be of the order

$$E\left[\frac{V}{m}\right] = \frac{2K[\text{eV}]}{R_0[\text{m}]}$$

The upper limit of deflecting 10 keV antiprotons, voltages in the kilovolt range were required.Changing voltages on these deflecting electrodes, one can tune the average energies of the particles seen by the detector. The requirements of the AEgIS collaboration are as follows. Needed are an antiproton beam with an average energy that can be tuned in the range of energies from 100 eV up to 10 keV. This is neccessary for the Talbot-Lau interferometry which will be used to determine the sign of g for antimatter. This is also ideal for demonstrating wavelike properties, the secondary goal of the collaboration. A high flux of particles is preferable to a monochromatic beam. Finally, the standard deviation of rms energies would ideally not exceed 10% of the rms energy.

The result of the research (picture in figure 1) was a tunable device 1 m $\times$ 0.5 m which has the predicted ability to deflect certain low energy ranges from a higher energy antiproton beam. The extractor consists of a cylindrical vacuum chamber with a y-junction. The low energy antiprotons are deflected from the main beam path at a 40 o angle. The internal geometry of the deflector begins with a collimator $10cm$ long with outer radius of 6 cm and inner radius of 3 cm. Next is the first of two einzel lenses the has a small inner

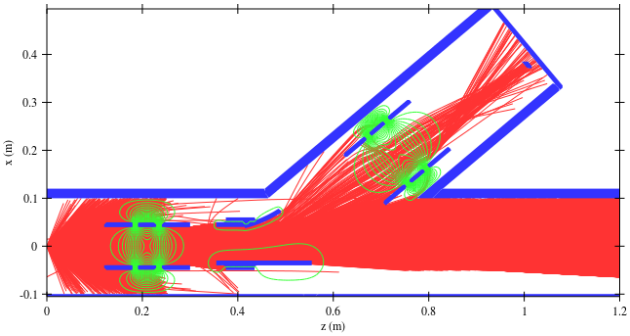


(a) Cutaway view of GRACE extracting antiprotons.

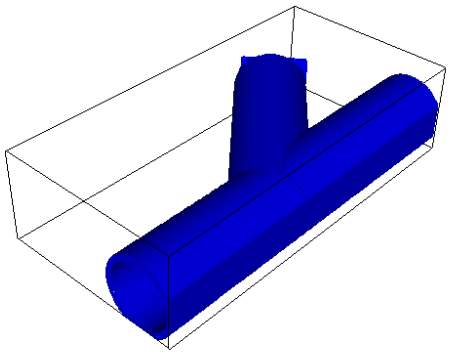

(b) Outside geometry of GRACE.

Figure 1: Final geometry for GRACE, the low-energy antiproton beam extractor which will provide antiprotons for capture in Penning trap. Blue corresponds to object boundaries which are defined by Dirichelet boundary conditions, green curves are electric equipotentials, and red lines are antiproton trajectories.

radius of $4cm$ and the second has a larger radius of 10 cm, in order to focus the more diffuse beam.

# Chapter 2: Theory

## Penning Trap Physics

The antiprotons extracted from GRACE will need to analysed and characterised. One way to do this is through the application of a Penning trap system for capturing the particles and studying their behavior and make measurements.[4] The motivation for a study of the dynamics of a particle in an Penning trap system. In order to fully characterise the beam extracted by GRACE a Penning trap is introduced to the system in order to analysis the properties of the cold antiprotons as they are extracted from the post-degraded beam extracted GRACE antiproton beam. The motion inside the trap must be well understand so a discussion of the physics of the Penning trap in the following section is necessitated. The discussion will use the formalism of the geonium atom.[3]

Since the antiprotons will be well below the relativistic energies, first the classical motion will be described. The particle of choice is an antiproton with charge $Q = q_p = q_e = e$ and mass $m_p$ in an approximately spatially uniform magnetic field. The cyclotron frequency of the particle, a useful value will be given by

$$\omega_c = \frac{|eB|}{m_p}$$

And using an appropriate value of 0.25 Tesla gives

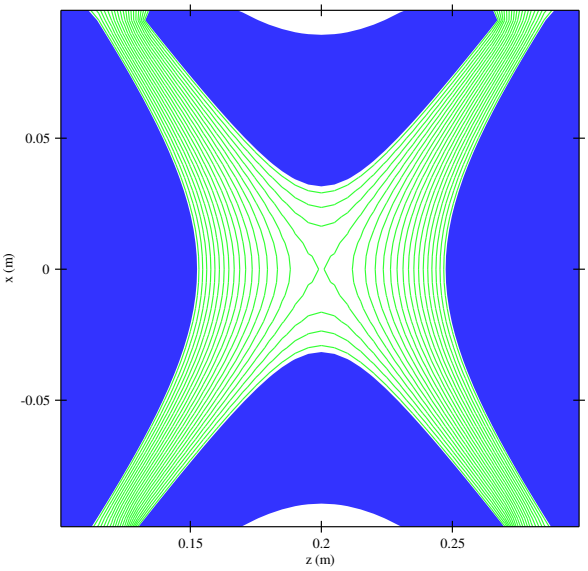


Figure 2: Here is a plot of a cross section of an ideal quadrupole, so $V = V_0 \frac{z^2 - \rho^2/2}{2d^2}$. Note that the hyperbolas are indeed on equipotential lines (the green contour curves). The two pairs of opposite electrodes were defined as hyperbolas with the following equations: $(y/0.1)^2 + (x/0.1)^2 - (z/0.075)^2 >= 0.1$ and $(y/0.1)^2 + (x/0.1)^2 - (z/0.075)^2 <= -0.4$

$$f_c = \frac{|eB|}{2\pi m_p} \approx 3.8\text{MHz}$$

A further discussion of additional parameters necessary to know for building a successful trap will be discussed later in the paper. For now however, the discussion will deal with the electric setup in an ideal Penning trap. Ideally, a Penning trap uses an electric quadrupole field, i.e.

$$V = V_0 \frac{z^2 - \rho^2/2}{2d^2}$$

Where $\rho$ is the radial coordinate. And note that only transverse motion is confined since the magnetic field is axial, in the $\hat{z}direction$. Again since in the ideal case, the three required electrodes would be setup along the equipotentials of a quadrupole so would consist of 2 hyperbolas of revolution, one concave and the other convex as depicted as depicted in the figure below.

The two endcap electrodes and ring hyperbola give a the following fields respectively

$$z^2 = z_0^2 + \frac{\rho}{2} \qquad\qquad z^2 = \frac{1}{2}\left(\rho^2 - \rho^2\right)$$

Where $z_0$ and $\rho_0$ denote the minimum axial distance and radial distance to the electrodes, respectively. The potential difference between the trap electrodes can be set to $V_0$ by saying $d = 0.5(z_0^2 + \rho_0^2/2)$ Since the particle is free to wobble in the axial direction itself. This motion is however, confined and oscillatory when $eV_0 > 0$. And the axial motion can be described by the following equation.

$$\ddot{z} = \omega_z^2 z = 0 \qquad \text{where} \qquad \omega_z^2 = \frac{eV_0}{md^2}$$

Typically $\omega_z << \omega_c$ so $\omega_z$ can usually be ignored. When the potential from the electrostatic elements is

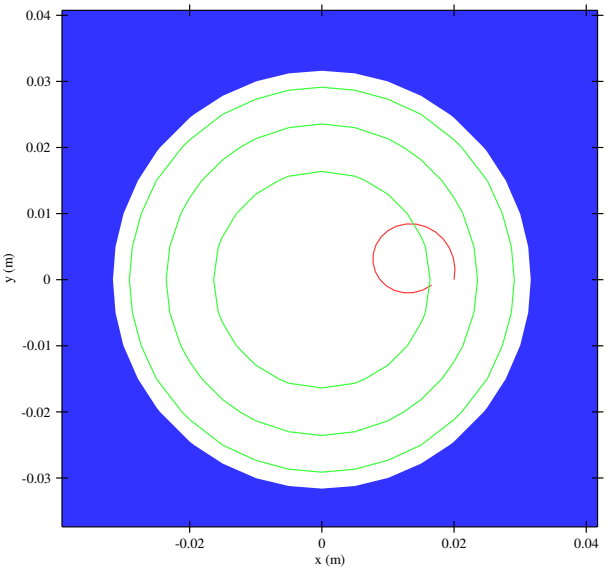


Figure 3: In the plot to the left is the trajectory of one period of cyclotron oscillation, $\omega_c$.

added the motion is described by

$$m\ddot{\rho} = e\left[\mathbf{E} + \left(\frac{\rho}{c}\right) \times \mathbf{B}\right] \qquad \text{where} \qquad \mathbf{E} = \left(\frac{V_0}{2d^2}\right)\rho$$

The particle's equations of motion in terms of the $z - oscillation$ and the cyclotron frequency is thus

$$\ddot{\rho} - \omega_c \times \dot{\rho} - \frac{1}{2}\omega_z^2 \rho = 0 \implies \ddot{\rho} - \omega_c \times \dot{\rho} \approx 0$$

In this approximation where $\omega_c = 0$ the equation of motion is that of uniform circular motion. There is however another magnetron oscillation called $\omega_m$ caused by the repulsive radial potential potential. In general the motion of the particle in the ideal Penning trap is that of the superposition of these three oscillations. From the results above the magnetron motion is given by

$$\omega_m \approx \frac{\omega_z^2}{2\omega_c}$$

So in general and without loss of generality it is true that, $\omega_m << \omega_z << \omega_c$. We can see that the typical values for a proton-mass particle are around 660kHz, 10 MHz, and 76 MHz. Critically, the axial and cyclotron motions are stable, the cyclotron motion is almost completely kinetic, the axial alternated between kinetic and potential as an oscillator, but the magnetron motion is almost entirely potential energy dependent. Exciting the particle in this motion will cause the particle to quickly roll escape in the radial direction. Thankfully though, the time scale of this loss is typically on the order of years so magnetron motion is metastable.[3]

Now to solve the previous equation of motion analytically it becomes necessary to separate cyclotron and magnetron motion by introducing the vector notation $\mathbf{V}^{\pm} = \dot{\rho}\omega_{\pm}\hat{z} \times \rho$ where

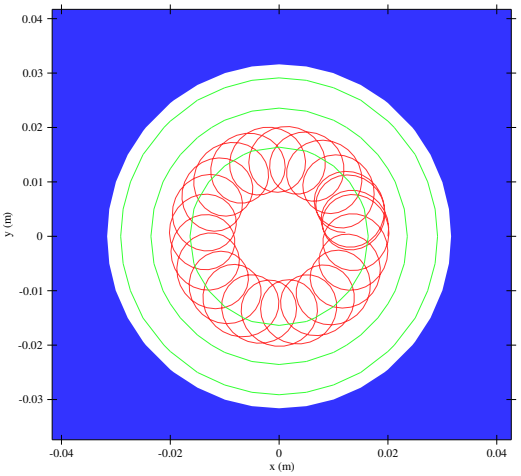


(a) The trajectory of one period of magnetron oscillation, $\omega_m$.

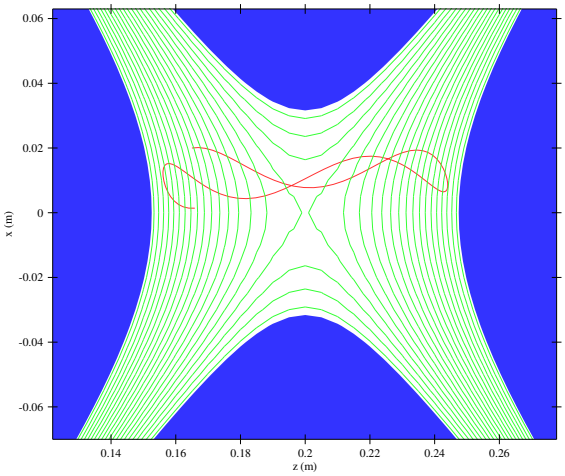


(b) The trajectory of one period of axial oscillation, $\omega_z$

Figure 4: Plots of one period of each of the three main degrees of oscillation. The trajectories are calculated for a proton-mass particle in an ideal hyperboloid quadrupole Penning trap with a constant magnetic field of, 0.25 Tesla in the axial direction.

$$\omega_\pm = \frac{1}{2}\left[\omega_c \pm \sqrt{\omega_c^2 - 2\omega_z^2}\right]$$

Now taking the time derivative of $\mathbf{V}^\pm$ gives

$$\dot{\mathbf{V}}^\pm = \omega_\pm \hat{z} \times \mathbf{V}^\pm$$

So from this it can be seen that $V^+$ rotates at the cyclotron frequency with a correction due to the magnetron motion, which will be called $\omega_c'$ . Since $\omega_+ + \omega_- = \omega_c$, then it is true that

$$\omega_+ = \omega_c' = \omega_c - \omega_m$$

And since $\mathbf{V}^-$ rotates at the magnetron frequency $\omega_m$ and since $\omega_+\omega_- = \omega_z^2/2$, the results show that

$$\omega_c = \omega_m = \frac{\omega_z^2}{2\omega_c'}$$

This difference $\mathbf{V}^+ - \mathbf{V}^-$ is proportional to $\hat{z} \times \rho$ which implies that

$$\rho = -\frac{\hat{z} \times (\mathbf{V}^+ - \mathbf{V}^-)}{\omega_+ - \omega_-} \implies \dot{\rho} = -\frac{\omega_+\mathbf{V}^+ - \omega_-\mathbf{V}^-}{\omega_+ - \omega_-}$$

The Hamiltonian for the radial motion, $\mathcal{H}_\rho$, is the sum of the kinetic energy and the electrode repulsion so

$$\mathcal{H}_\rho = \frac{m}{2}\left(\dot{\rho}^2 - \frac{1}{2}\omega_z^2\rho^2\right)$$

Which can be combined with our previous results to get that

$$\mathcal{H}_\rho = \frac{m}{2}\frac{\omega_+\left(\mathbf{V}^+\right)^2 - \omega_-\left(\mathbf{V}^-\right)^2}{\omega_+ - \omega_-}$$

An interesting feature to note is that the magnetron motion gives a negative contribution to the energy since it is inherently unstable motion. Now it is necessary to take into account radiation damping, since the charged particle is in fact accelerating within the trap. First note the usual expression for the Larmor formula.[3]

$$-\frac{dE}{dt} = \frac{2e^2}{3c^3}\ddot{\rho}^2 \qquad \text{where} \qquad \ddot{\rho} = \omega_c \times \dot{\rho} \qquad \text{and} \qquad E = \frac{1}{2}m_p\dot{\rho}^2$$

$$\implies \frac{dE}{dt} = -\frac{4e^2\omega_c^2}{3mc^3}E \implies \frac{dE}{E} = -\frac{4e^2\omega_c^2}{3mc^3}dt$$

And if the definition $\gamma = \frac{4e^2\omega_c^2}{3mc^3}$ is made then the energy decays with the exponential relation

$$E(t) = E_0 e^{-\gamma t}$$

Thankfully, for an antiproton, putting in appropriate values. the radiation damping time due to cyclotron motion is on the order of $\approx 10^8$ seconds and is thus insignificant. Smaller particles such as electrons would be much harder to contain. The results can be verified with a more exhaustive quantum mechanical treatment using transition probabilities but it contributes little knew relevant insight to the problem at hand. Now, this analysis has all be done using the ideal Penning trap with quadrupole fields from hyperbolic electrodes. In the proposed permanent magnet design an axially cylindrical trap with compensator electrodes is used, so a discussion of difference is needed for later in the report.

## Permanent Magnet Penning Traps

Typical Penning traps used for antimatter, nuclear spectrometry, or other nuclear research projects require superconducting solenoids to generate the necessary axial magnetic field, on the order of several Tesla.[11] As a resulted, a large amount of additional apparatus is necessitated for cooling purposes. Large cryostats for example lead to the case where a high magnetic field Penning trap is a large and costly device.[12]

This is not desirable, so alternatively, a Penning trap design using rare-earth magnets is much more desirable. The magnetic fields are often only 1 or 2 Tesla but are much more versatile.[12] There exist precedence for compact traps with magnetic fields generated by wedges of NdFeB in the 50 to 100 Kelvin range[12] and other work established created axial magnet arrays with epoxy bonded radially-magnetized segments was used to store anions at room temperature.[26] In order to trap the desire low-energy antiprotons from

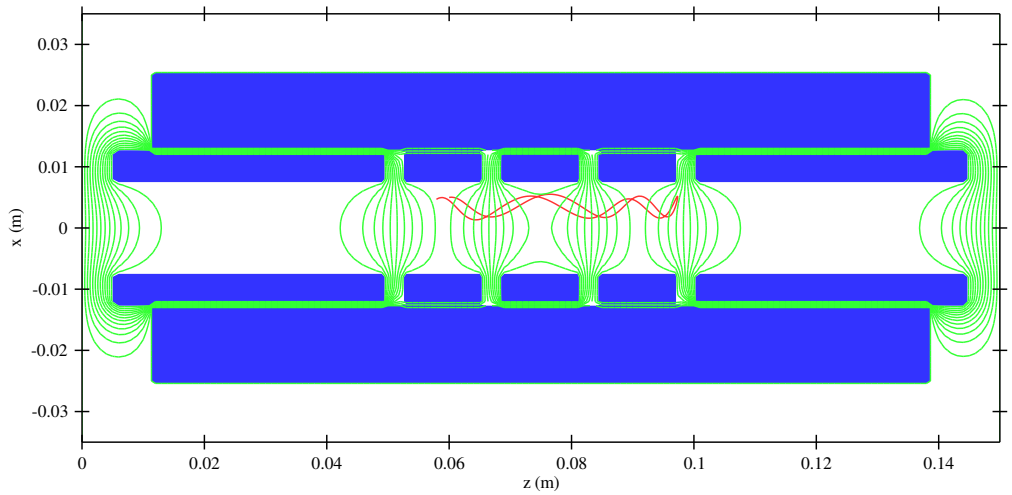


Figure 5: The trajectory of one period of axial oscillation, $\omega_z$

the GRACE beam extractor, an axial Penning trap has been designed which uses an array of ring magnets concentric with the cylindrical electrodes.

The design is of an open-access orthogonalized Penning trap.[9] The design allows axial access needed to capture antiprotons which were not well localized as they arrived to the trap. At the same time, it provides an environment for one trapped antiproton allowing for measurements to be made on it. After antiprotons are captured, their number can be carefully reduced until only one remains and indeed manipulated with the compensator electrodes. A careful choice of the potentials of the ring electrodes controls the desired "orthogonalized" behaviors. In this behavior, the axial frequency of the antiproton is almost entirely independent of the compensation potential that is tuned to make the trap more harmonic.[9]

As a comparison to the ideal quadrupole trap, the same oscillation periods are found in the axial trap and plotted in the figures 5 and 6. It is found indeed that the cyclotron frequency remains almost exactly the same, further encouraging the constant magnetic field approximation. However, the axial and magnetron frequencies are not unchanged. The axial frequency is decreased by a factor of two, while the magnetron frequency is decreased by a factor of four.

# Chapter 3: Simulations

## IBSimu

In order to make the particle dynamics simulations easier Ion Beam Simulator (IBSimu) was used.[19] It is a highly versatile C++ library used for ion optics simulations. The libraries can be used for both 2D and

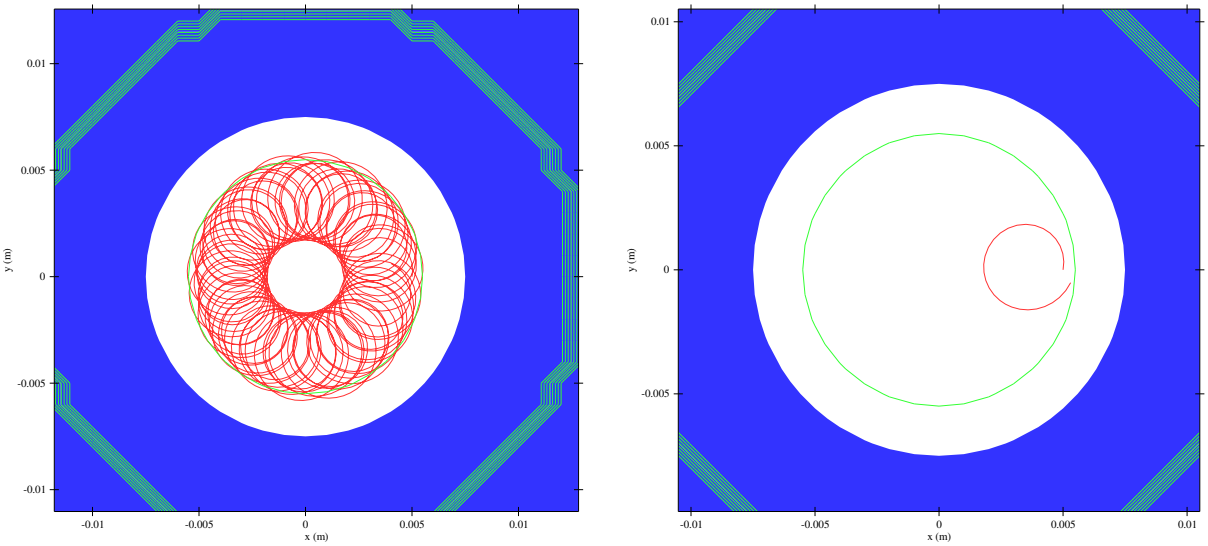


(a) The trajectory of one period of magnetron oscillation, $\omega_m$.

(b) In the plot to the left is the trajectory of one period of cyclotron oscillation, $\omega_c$.

Figure 6: Plots of one period of each of the three main degrees of oscillation. The trajectories are calculated for a proton-mass particle in an ideal hyperboloid quadrupole Penning trap with a constant magnetic field of, 0.25 Tesla in the axial direction.

3D simulations in a transparent and user friendly manner. Within the structure of the library, solids can be defined using mathematical descriptions to create Boolean functions which are then used as boundary conditions for field solutions. The domain of the simulations is a discretized rectangular mesh with a constant step size.[20] In order to calculate the necessary potentials, the libraries have methods to solve Poissons equation

$$\nabla^2\phi = \frac{-\rho}{\epsilon_0}$$

using finite difference methods on the nodes of the mesh. In order to smooth the electric fields on the edges of defined solids, the nodes on the edges are adjusted to virtual potentials using subnode geometry information. The edges can further be defined with Dirichlet or Neumann boundary conditions (i.e. first and second order approximations). Furthermore, the most appealing aspect of the library is that it can support the well-established nonlinear plasma model for ion extraction. Furthermore, the library has multiple nonlinear solvers for calculating electrostatic potentials.

For the 3D simulations, a biconjugate gradient stabilized (BiCGSTAB) method was used for solving for the scalar fields.[19] The method is a modification of the biconjugate gradient method which is faster and smoother in its convergence. The later is an algorithm used to solve non symmetric linear systems of equations. We start with a linear system $Ax = b$ and an initial guess of $x_0$ .
From this our algorithm is given as follows:[6][24]

1. $r_0 = b - Ax_0; r_0$ arbitrary with $(\bar{r}_0, r_0) \neq 0$
2. $p_0 = r_0$
3. for $j = 0, 1, 2, 3...$ until convergence
   (a) $\alpha_j = (r_j, \bar{r}_0)/(Ap_j, \bar{r}_0)$
   (b) $s_j = r_j - \alpha_j Ap_j$
   (c) $\omega_j = (As_j, s_j)/(As_j, As_j)$
   (d) $x_{j+1} = x_j + \alpha_j p_j + \omega_j s_j$
   (e) $r_{j+1} = s_j - \omega_j As_j$
   (f) $\beta_j = (r_{j+1}, \bar{r}_0)/(r_j, \bar{r}_0) \cdot \alpha_j/\omega_j$
   (g) $p_{j_1} = r_{j+1} + \beta_j(p_j - \omega_j Ap_j)$
4. end for

The particle trajectories are calculated by integrating the equations motion derived from the Lorentz force using a Runge-Kutte Cash-Karp method (going up to fifth order). Furthermore, there exist in the library, methods to automatically adjust the step size in order to adjust for sufficient trajectory accuracy in more complicated fields. The Runge-Kutte method used is derived from the GNU Scientific Library[19]. Furthermore, the particle trajectory calculations are multithreaded[19] in order to increase the efficiency of calculations on a multicore CPU.

The algorithm for particle trajectories further finds all the mesh nodes the particle passes through and deposits that particles charge on the eight adjacent nodes and also checks for particle collisions in the mesh. This functional can and is suppressed for the simulations of the antiprotons in thePenning trap here since we are not examining collision aspects. In addition, particle trajectories area automatically terminated when hitting the defines boundaries, both Dirichelet and Von Neumman, corresponding to annihilating on the trap and escaping out of the bounds of the evaluation box respectively.

Going back to particle trajectory calculations, the electric field needed for particle trajectory calculation is obtained by numerical differentiation and interpolation of potential the potential taking into account the 27 nearest mesh nodes, special additional methods are used to adjust for mesh nodes close by to the boundaries of solids and the simulation box. As a result, the electric field is continuous everywhere in the simulation. Magnetic fields are imported from external calculation, as discussed in the next section, or, where appropriate defined by a simple vector field array with appropriate for loops.

## Magnetic Fields

The ideal magnetic field used for the Penning trap design would be constant and in the axial direction. This precise ideal field is impossible in realizable geometries so an approximation is attempted, beginning by calculating the analytic field of a cylindrical permanent magnet along the axis of symmetry. Noting Ampere's law in vacuum implies that $\nabla \times \mathbf{H} = 0$. Since current density $\mathbf{J} = 0$. So $\mathbf{H}$ can be written as the negative gradient of a potential, $\Phi$. More specifically,

$$\mathbf{H} = -\nabla\Phi$$

Furthermore, $\Phi$ will satisfy Poissons equation and the magnetic flux continuity law says that $\nabla \cdot \mu_0\mathbf{H} = -\nabla \cdot \mu_0 M$, so it follows that

$$\nabla\Phi = -\frac{\rho_m}{\mu_0} \qquad \text{where} \qquad \rho_m = -\nabla \cdot \mu_0 \mathrm{M}$$

So if a magnetization density is specified, a magnetic charge density $\rho_m$ can be determined. And since the net magnetic charge of a magnet is 0.

$$\int_V \rho_m dv = \oint_S \mu_0 \mathbf{H} \cdot d\mathbf{a} = 0$$

The integral can be evaluated over the volume which contains the permanent magnet. This is given by the integral representing the superposition due to all magnetic charges, such that

$$\Phi = \int_V \frac{\rho_m(\mathbf{r}')dv}{4\pi\mu_0|\mathbf{r} - \mathbf{r}'|}$$

So for a uniformly magnetized cylinder in the z-direction (axial direction), $\mathbf{M} = M_0\hat{\mathbf{z}}$. In the volume of the magnet, the $\mathbf{M}$ is constant so divergence-less. So the source of $\mathbf{H}$ is only on the surface where $\mathbf{M}$ originates. So it is true that

$$\sigma_{sm} = -n \cdot \mu_0(\mathrm{M}^a - M_b) = \pm\mu_0 M_0$$

So, where $d$ is the length of the cylinder along $z$, the integral becomes

$$\Phi = \int_0^R \frac{\mu_0 M_0 2\pi\rho' d\rho'}{4\pi\mu_0\sqrt{\rho' + (z-d)^2}} - \int_0^R \frac{\mu_0 M_0 2\pi\rho' d\rho'}{4\pi\mu_0\sqrt{\rho' + (z+d)^2}}$$

$$= \frac{dM_0}{2}\left[\sqrt{\left(\frac{R}{d}\right)^2 + \left(\frac{z}{d}\right)^2} - \sqrt{\left(\frac{R}{d}\right)^2 + \left(\frac{z}{d}\right)^2}\right]$$

From which the gradient is taken to obtain

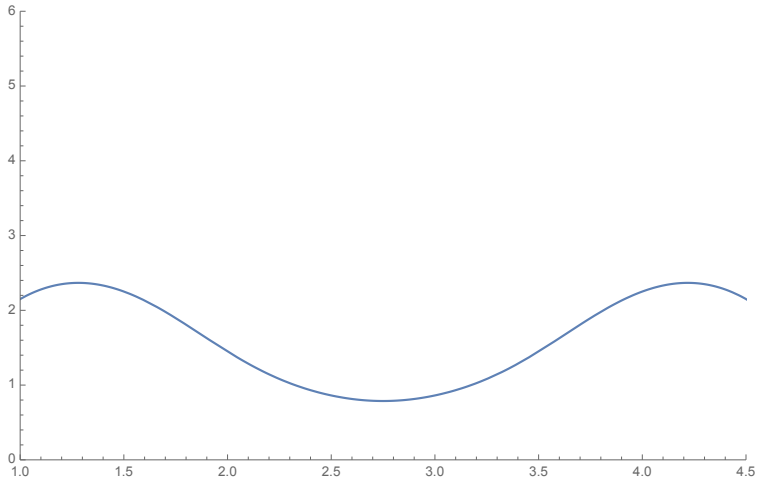


Figure 7: ... caption text ...

$$H_z = -\frac{dM_0}{2}\left[\frac{z/d - 1/2}{\sqrt{\left(\frac{R}{d}\right)^2 + \left(\frac{z}{d}\right)^2}} - \frac{z/d + 1/2}{\sqrt{\left(\frac{R}{d}\right)^2 + \left(\frac{z}{d}\right)^2}}\right]$$

Thus

$$\mathbf{B}_z = \frac{B_r}{2}\left[\frac{z - D}{\sqrt{\left(\frac{R}{d}\right)^2 + \left(\frac{z}{d}\right)^2}} - \frac{z + D}{\sqrt{\left(\frac{R}{d}\right)^2 + \left(\frac{z}{d}\right)^2}}\right]\hat{\mathbf{z}}$$

Since this is the magnetic field for one cylindrical permanent magnet in order to find the fields of a hollow cylindrical magnet we take the superposition of this field and another cylindrical magnet of the inner radius but with fields in the opposite direction to get the magnetic field along the axis of an axially magnetized hollow cylinder as[18]

$$\mathbf{B}_z = \frac{B_r}{2}\left[\frac{z - D}{\sqrt{\left(\frac{R}{d}\right)^2 + \left(\frac{z}{d}\right)^2}} - \frac{z + D}{\sqrt{\left(\frac{R}{d}\right)^2 + \left(\frac{z}{d}\right)^2}} - \left(\frac{z - D}{\sqrt{\left(\frac{R}{d}\right)^2 + \left(\frac{z}{d}\right)^2}} - \frac{z + D}{\sqrt{\left(\frac{R}{d}\right)^2 + \left(\frac{z}{d}\right)^2}}\right)\right]\hat{\mathbf{z}}$$

In order to build up the magnetic array on the external portion of our electrodes, it is then rather trivially take these magnets and again take the superposition to get the total field due to an array of axially magnetized rings along the axis, a procedure which is undertaken in Mathematica and plotted below.

From this one can conclude two crucial pieces of information, first of all one can see that it is possible to predict the minimum B field inside the trap (which will be along the z-axis) and also are able to make sure the scaling is correct in a 2D ViziMag simulation. Two-dimensional simulations are much easier than 3D simulations and the functional form will be the same since their is rotational symmetry, the only problem could be rescaling which will be accomplished with the analytic results.

As alluded to, 2D simulations of magnetic field strength were carried out using ViziMag. The axis field of the trap is constant approximately an inch into the trap, which is suitable for our simulations.

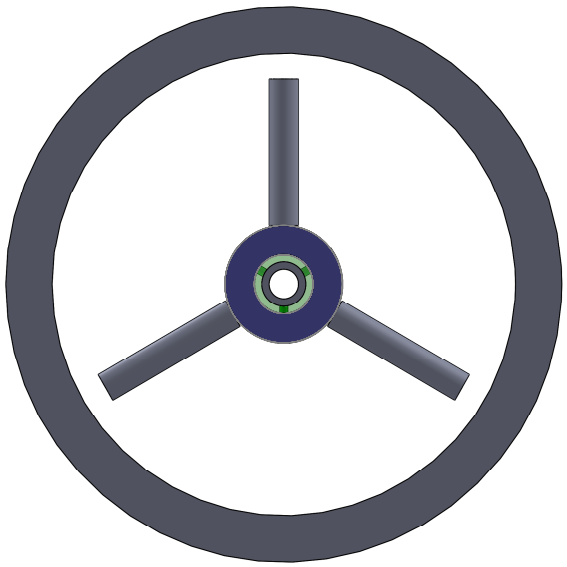

(a) View of Penning trap design along z-direction.

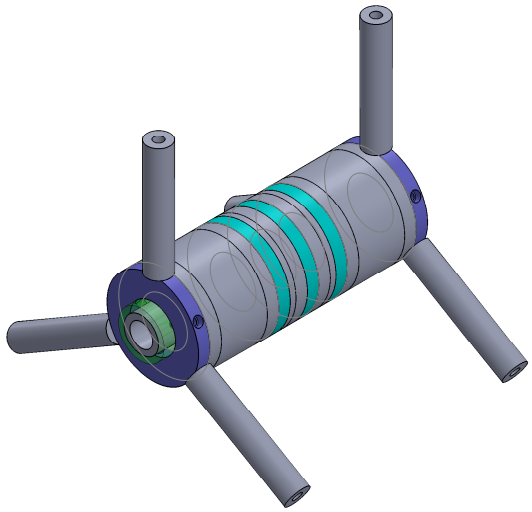

(b) Isometric view of Penning trap design with stand off struts to be used for mounting and position in vacuum chamber

Figure 8: Two different views of Penning trap geometry made in SolidWorks. The different colors correspond to different materials which are

### Simulations

# Chapter 4: Manufacturing and Design

## Manufacturing

To reiterate, the design is for an axially oriented cylindrically symmetric Penning trap, the easiest to manufacture as well as the best for capturing antiprotons traveling with predominant z-direction velocity.

The base of the design is of a series of 5 cylindrical cylindrical electrodes concentrically mated to the inside of column of ring magnets to establish a nearly constant magnetic field. The external magnet array is composed of 30inch0.125 inch thick ring magnets with 1 inch in ID and 2 inches in OD. They are N42, NdFeB magnets. The arrangement is depicted in figure 8.

The open ends allow a number of advantages, first of all, the open entrance allows capturing the post GRACE antiprotons. And the open exit allows the escape of trapped particles for measurement with the MCP, see chapter 5. The the inner tube is composed of two layers, the outer layer is a solid plastic tube with 5 clearance holes drilled through to allow access to the inner electrodes and 6 more to allow access for the stabilization screws. The inner tube consists of the five electrodes, and four additional plastic spacers to isolate the electrodes. The outer two electrodes have two holes to attach to the mounting pieces. The bolt

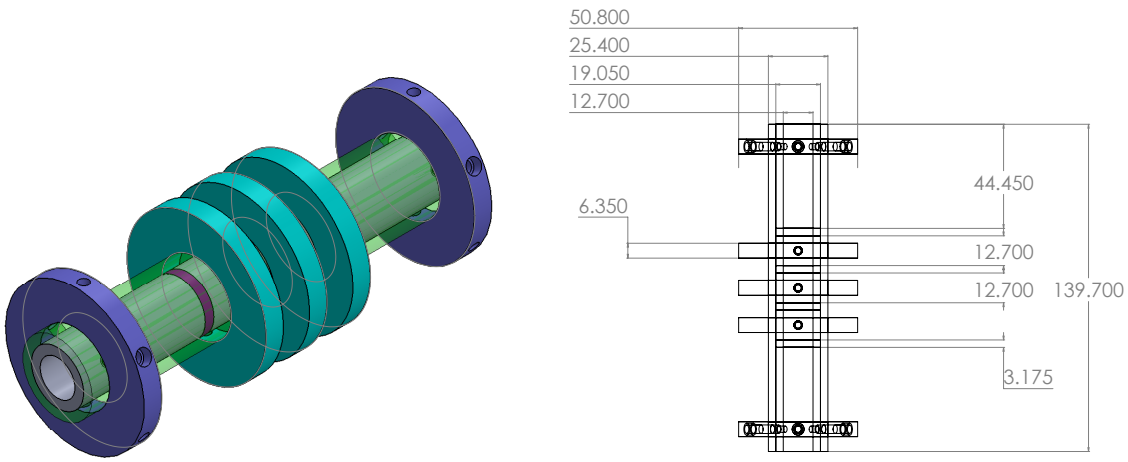


(a) (b)

Figure 9: Penning trap design with stand offs and ring magnets suppressed. All distances are measure in mm.

sizes will be 6-32 and the sizes of clearance holes will be large enough for these bolt sizes. The dimensions are apparent in figure 9.

The access rings are also made out a stainless steel, the best available stock and easiest to machine clearance holes into, the outer mounting rings are made from stainless steel and have 6 holes, 3 for mounting through insulating tube into the outer electrodes and 3 for attaching to the adjustable stand-offs. These also fill the role of keeping the magnets and accessing elements axially located on the tube. Each outer mount has three standoffs with an isolating screw on the outside for fin adjustment in the vacuum chamber. In addition, the inner outer electrodes and the insulating tube have a quarter inch of extra length outside of the trap magnets. A material which prevents charge build up is preferable so we choose to make the insulating tube out of acrylic due to its tendency to avoid charge build up. The dielectric strength of acrylic is[14]

$$17 \text{ kV/mm} \implies 17 \text{ MV/m}$$

And the dielectric strength of extruded teflon is 19.7 MV/m[13], again more than enough to avoid dielectric breakdown. The electrode voltage required is only on the order of hundreds of volts. The bolts will be vacuum safe and locktight will be used to hold them together. The trap is thus reduced to the machining of 21 parts, 5x connectors, 6 stand offs, 5 electrodes,1 insulating tube, and 4 insulating spacers. The critical detail is the order of assembly. The connections to the electrode will be established before insertion into the tube. The first stand off connector will be attached to the insulating tube, then the electrodes will placed inside and threaded through the appropriate insulating tube holes. Then the first 12 magnets on the

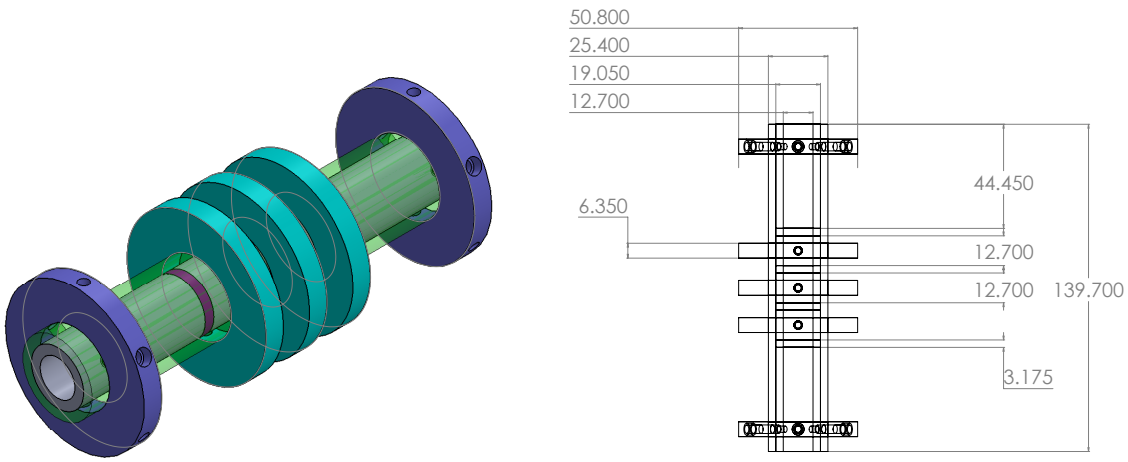


(a) (b)

Figure 10: Penning trap design with stand offs and ring magnets suppressed. All distances are measure in mm.

outside, then the first connector the voltage wire pulled through the hole, then the next 3 magnets, the next connector and so on and so forth until the last end cap. See figure 10. The design will be manufacturing in the BU Scientific Instrumentation Facility.

### Use in Trap/Interfacing with GRACE

The data used as input was briefly alluded to for the simulations from chapter 2, but it is here that the details are explained. The work with GRACE established the positions in phase space of the low energy antiprotons which could be extracted. The previous data was used to establish the appropriate phase space of particles to add to the Penning trap simulation and then use a pseudorandom number generator in order to simulate a large number of appropriate particles. Statistics could then be made regarding the percentage of particles trapped. Of 100000 trials of potentially trapped particles (under 10keV), 19981 were captured for more than 1 second. This corresponds to a simulated $\approx 20\%$ catch rate. Histograms of the input and output energies are given in the figure below.

## Chapter 5

### Testing the Apparatus

Before, attempts are made to capture antiprotons directly, it is helpful to test the apparatus with a less costly ion source. An electron cathode ray source would be the easiest source but it has already been shown that the lifetime an electron in the trap is far too short due to radiative cooling for accurate measurements

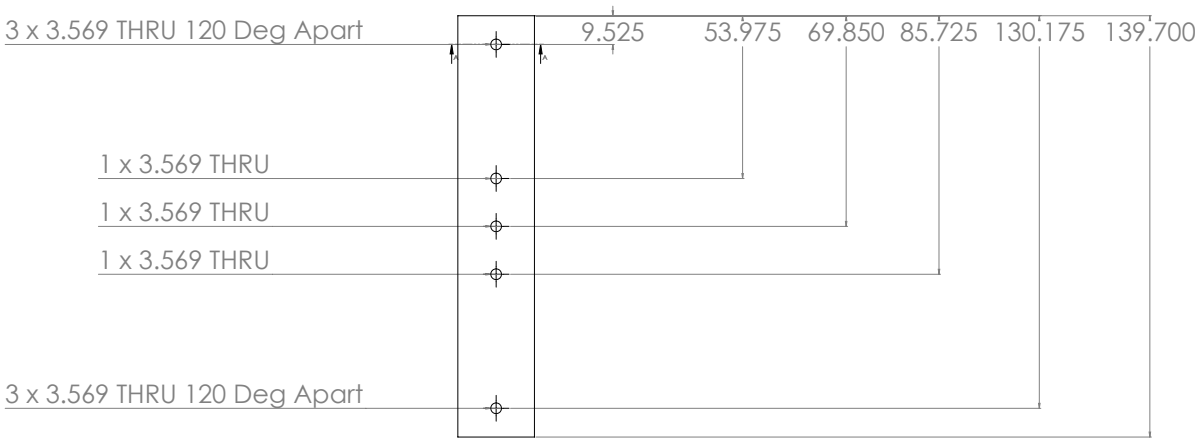


Figure 11: Acryclic tube spacer to isolate the electrodes from the neodymium magnets and the support structures.

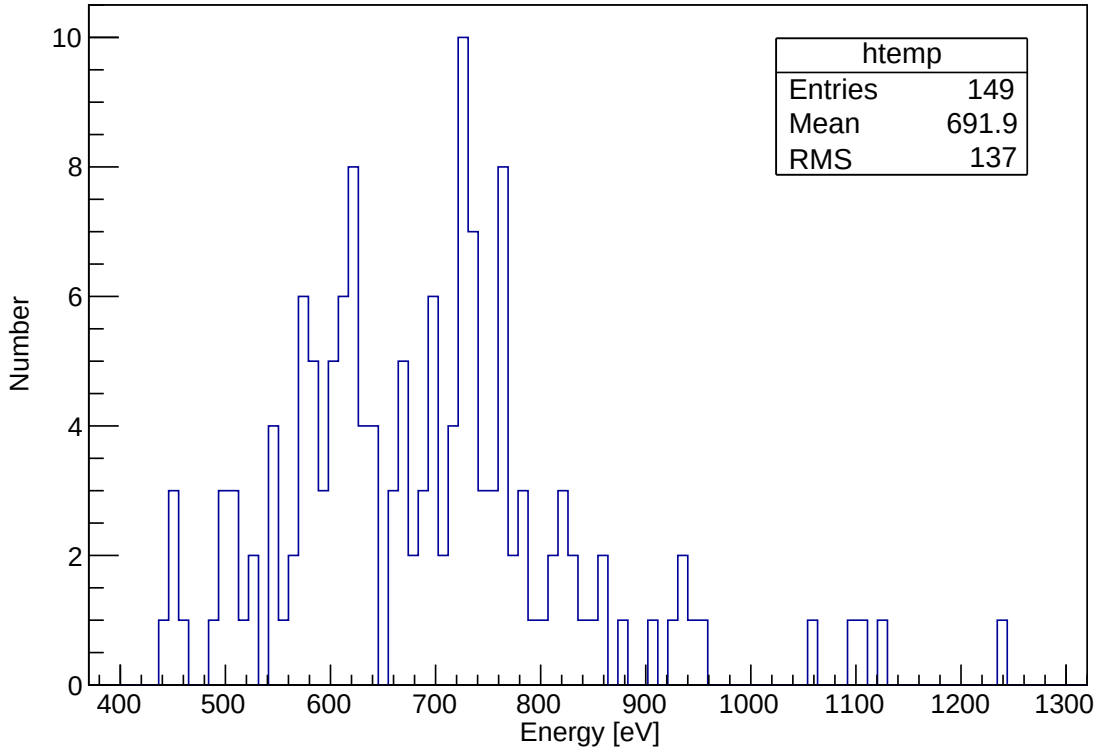


Figure 12: Caught antiprotons

Figure 13: Histograms of output antiproton from GRACE simulations (particles which hit a $2mm \times 2mm$ detector).

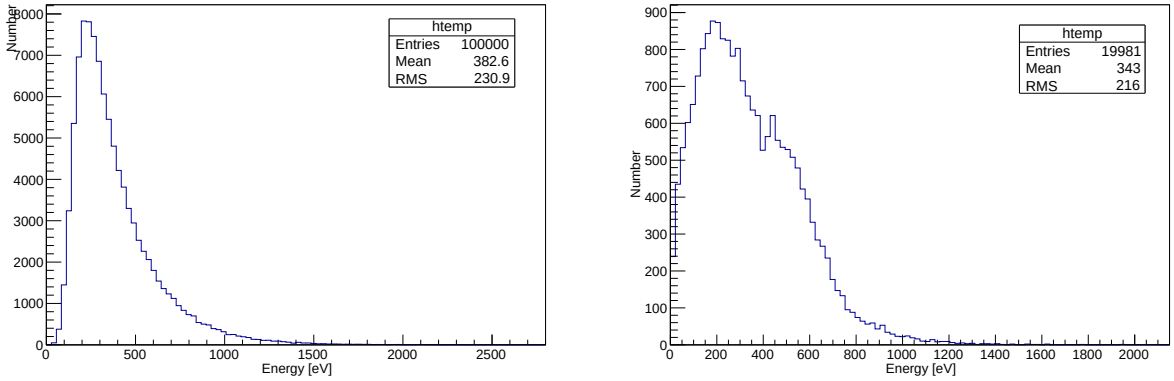


(a) Input antiprotons

(b) Caught antiprotons

Figure 14: Histograms of input antiprotons total energy and energy of antiprotons caught for greater than one second.

to be made. Instead using a heavy ion source would be preferable. In order to measure the presence of the particles in the trap, they must be dumped them by shutting off the fields and measuring the output with an MCP. First of all, an MCP is a microchannel plate detector, a device made of a very dense stack of millions of electron multiplier tubes. The detector we intend to use is the one which tubes of diameters on the order of 10 micrometer. and lengths on the order of 1 mm. A relevant quantity is the length-to-diameter ratio which in this case is 100. The distance between tubes is only slightly larger than the tube diameters.

In order to use appropriately a heavy ion source, a series of degrader foils will be necessary, the most convenient being aluminum degrader foil, simulations are performed with SRIM (The Stopping and Range of Ions in Matter) in order to gain a approximate quantitative knowledge of the thickness of degrader foil required. SRIM is a free open source program used to simulate and predict the stopping range of ions in a variety of types of matter. This is necessitated because any ion source would be generating a number of particles too high to be caught by the Penning trap. The results of these simulations are contained within the appendix, but suffice it to say that the use of an ion hydrogen source would be ideal for testing the trap before accessing antiprotons. Indeed, the degrader aluminum foil should work quite well for a number of different energy ion sources.[2]

## Conclusions

Even with our modern understanding of physics, a number of mysteries remain. One place of particular interest is in the study of the nature of the mysterious substance called antimatter, and no doubt antimatter will continually be studied for many years to come. Indeed, at CERN, some of these great questions are being answered, including one of the most enduring questions is how to explain the asymmetrical amount of matter and antimatter in the universe.

The Antiproton Decelerator (AD), is an antiproton storage ring from which several international collaborative experiments obtain the antiprotons for their experiments. The AEGIS (Antimatter Experiment: Gravity, Interferometry, and Spectrometry) collaboration is a collaboration seeking to measure the weak equivalence principle of antimatter.[3] In previous work, a device was designed for Generating a Reduced-energy Antiproton Beam using Channeling Electrostatics (GRACE).[4] Its purpose is to extract an antiproton beam of tunable mean energy anywhere from 0.1 to 1 keV, from a beam of energies with an upper limit of 5 MeV. An ion trap (Penning trap) was designed to be placed at the end of the beamline in order to trap antiprotons to assess certain properties of the deflected particles. A study of particle dynamics relating to ion optics and beam physics was undertaken in order to understand the behavior of the particles. The studies helped accurately simulate particles in the trap in order to create an effective design and to ensure that in simulation, a sufficient number of antiprotons were captured and held for an sufficiently long time while avoiding instabilities which may cause a loss of particles.

Typical Penning traps used for antimatter, nuclear spectrometry, or other nuclear research projects require superconducting solenoids to generate the necessary axial magnetic field, on the order of several Tesla. As a resulted, a large amount of additional apparatus is necessitated for cooling purposes. Large cryostats for example lead to the case where a high magnetic field Penning trap is a large and costly device.[1] This is not desirable, so alternatively, a Penning trap deisgn using rare-earth magnets is much more desirable. The magnetic fields are often only 1 or 2 Tesla but are much more versatile.[1] There exist precedence for compact traps with magnetic fields generated by wedges of NdFeB in the 50 to 100 Kelvin range [2] and other work established created axial magnet arrays with epoxy bonded radially-magnetized segments was used to store anions at room temperature.[29] In order to trap the desire low-energy antiprotons from the GRACE beam extractor, an axial Penning trap has been designed which uses an array of ring magnets concentric with the cylindrical electrodes.

# References

[1] Aghion, Stefano, et al. "A moir deflectometer for antimatter." Nature communications 5 (2014).

[2] Amole, C., et al. "The ALPHA antihydrogen trapping apparatus." Nuclear Instruments and Methods in Physics Research Section A: Accelerators, Spectrometers, Detectors and Associated Equipment 735 (2014): 319-340.

[3] Brown, Lowell S., and Gerald Gabrielse. "Geonium theory: Physics of a single electron or ion in a Penning trap." Reviews of Modern Physics 58.1 (1986): 233.

[4] Blaum, Klaus, Yu N. Novikov, and Gnter Werth. "Penning traps as a versatile tool for precise experiments in fundamental physics." Contemporary Physics 51.2 (2010): 149-175.

[5] Chao, Alexander Wu, et al., eds. Handbook of accelerator physics and engineering. World scientific, 2013.

[6] Chen, Jie, Lois C. McInnes, and Hong Zhang. "Analysis and practical use of flexible BICGSTAB." Journal of Scientific Computing (2012): 1-23.

[7] Derby, Norman, and Stanislaw Olbert. "Cylindrical magnets and ideal solenoids." American Journal of Physics 78.3 (2010): 229-235.

[8] Doser, M., et al. "Exploring the WEP with a pulsed cold beam of antihydrogen." Classical and quantum gravity 29.18 (2012): 184009.

[9] Gabrielse, G., L. Haarsma, and S. L. Rolston. "Open-endcap Penning traps for high precision experiments." International Journal of Mass Spectrometry and Ion Processes 88.2 (1989): 319-332.

[10] Giammarchi, Marco G., and AEGIS Collaboration. "AEGIS at CERN: measuring antihydrogen fall." Few-Body Systems 54.5-6 (2013): 779-782.

[11] Gomer, V., Strauss, H., Meschede, D.: A compact Penning trap for light ions. Applied Physics B: Lasers and Optics 60, 8994 (1995). URL http://dx.doi.org/10.1007/BF01135848. 10.1007/BF01135848

[12] Guise, Nicholas D., Samuel M. Brewer, and Joseph N. Tan. "Highly Charged Ions in Rare Earth Permanent Magnet Penning Traps." New Trends in Atomic and Molecular Physics. Springer Berlin Heidelberg, 2013. 39-56.

[13] `http://www.aerocomfittings.com/electrostatic.html`

[14] `http://www.builditsolar.com/References/Glazing/physicalpropertiesAcrylic.pdf`

[15] `http://aegis.web.cern.ch/aegis/Prive/Docintern/Why.pdf`

[16] `http://www.ansto.gov.au/__data/assets/pdf_file/0019/50464/Sydney_talk_Michael_Doser.pdf`

References continued on next page... 

[17] http://math.ucr.edu/home/baez/physics/ParticleAndNuclear/antimatter_fall.html

[18] Kaenders, W. G., et al. "Pure multipoles from strong permanent magnets: analytic and experimental results." Hyperfine Interactions 76.1 (1993): 221-232.

[19] Kalvas, Taneli, et al. "IBSIMU: A three-dimensional simulation software for charged particle opticsa)." Review of Scientific Instruments 81.2 (2010): 02B703.

[20] Kalvas, T. "Beam Extraction and Transport." arXiv preprint arXiv:1401.3951 (2014).

[21] Kellerbauer, A., et al. "Proposed antimatter gravity measurement with an antihydrogen beam." Nuclear Instruments and Methods in Physics Research Section B: Beam Interactions with Materials and Atoms 266.3 (2008): 351-356.

[22] Menary, Scott. "Why We Already Know that Antihydrogen is Almost Certainly NOT Going to Fall" Up"." arXiv preprint arXiv:1207.7358 (2012).

[23] Moore, F. L. "Penning Trap Experiments at the University of Washington and at NIST in Boulder." (1991): 98-107. APA

[24] Saad, Yousef. Iterative methods for sparse linear systems. Siam, 2003.

[25] Storey, James William, and AEGIS collaboration. "Towards the production of an ultra cold antihydrogen beam with the AEGIS apparatus." Hyperfine Interactions 212.1-3 (2012): 109-116.

[26] Suess, L., Finch, C.D., Parthasarathy, R., Hill, S.B., Dunning, F.B.: Permanent magnet Penning trap for heavy ion storage. Review of Scientific Instruments 73(8), 28612866 (2002). DOI 10.1063/1.1490411. URL http://link.aip.org/link/?RSI/73/2861/1

# Appendix

## Ring Magnet Specifications

The ring magnets to be used are neodymium rare earth magnets, which are the strongest in the world. Neodymium magnets (also known as Neo, NdFeB, or NIB) are permanent magnets made from neodymium, iron, boron and other minor elements. The type to be used by the Penning trap, are grade N48, stronger than N45, N42, N40, N38 and N35. They have

$$B_r = 14200 \text{ Gauss} = 1.42 \text{ Tesla}$$

The dimensions of the N48 magnet are 2 inch OD x 1 inch ID x 1/8 inch thickness. The magnets have a nickel-copper-nickel triple layer coated for maximum durability and protection again corrosion. They are magnetized through the 1/8" thickness and have a pull force of approximately 27 lbs.

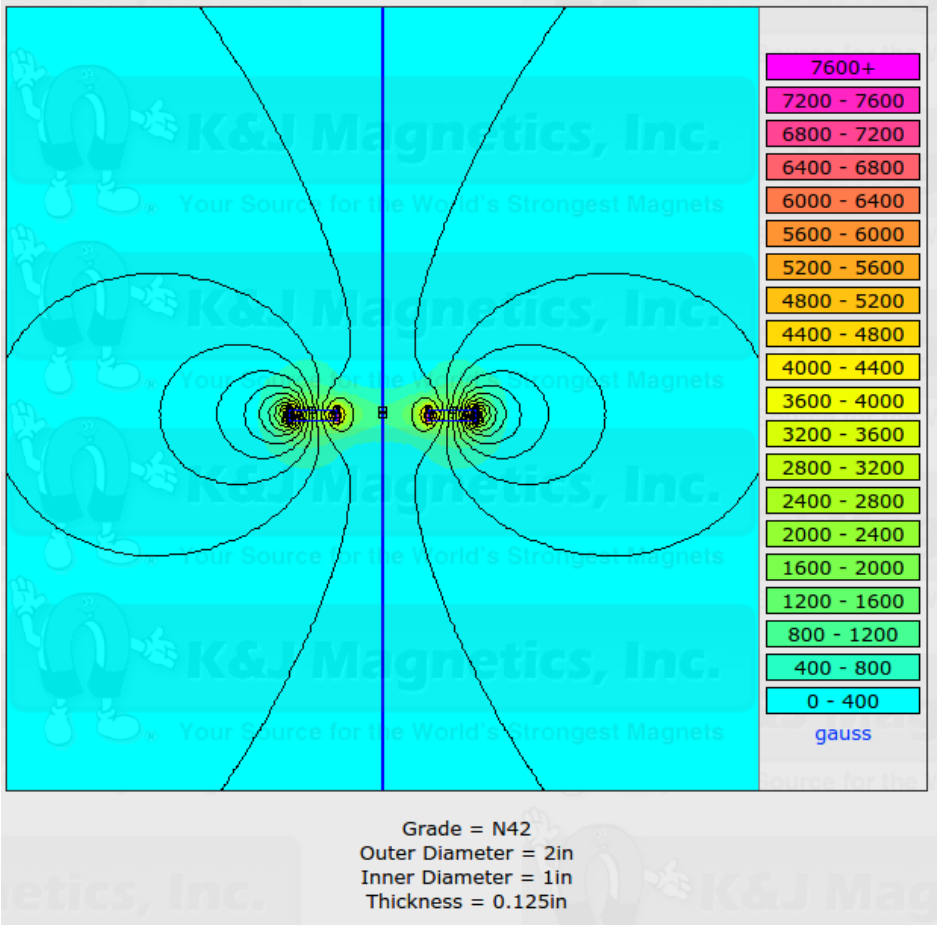


Figure 15

## SRIM Data Tables

```
==================================================================
               SRIM version ---> SRIM-2013.00
               Calc. date   ---> February 10, 2016
==================================================================

Disk File Name = SRIM Outputs\Hydrogen in Aluminum.txt
Ion = Hydrogen [1] , Mass = 1.008 amu
Target Density =  2.7020E+00 g/cm3 = 6.0305E+22 atoms/cm3
======== Target  Composition ========
   Atom    Atom    Atomic     Mass
   Name    Numb    Percent    Percent
   ____    ____    _______    _______
    Al      13     100.00     100.00
====================================

Bragg Correction = 0.00%
Stopping Units =  MeV / (mg/cm2)
See bottom of Table for other Stopping units
      Ion          dE/dx        dE/dx      Projected   Longitudinal    Lateral
     Energy        Elec.        Nuclear      Range      Straggling    Straggling
 _____________  __________ __________ __________  __________  __________
 10.00 keV    2.797E-01  4.085E-03    1277 A       501 A       471 A
 11.00 keV    2.924E-01  3.861E-03    1382 A       518 A       493 A
 12.00 keV    3.044E-01  3.664E-03    1484 A       534 A       514 A
 13.00 keV    3.155E-01  3.489E-03    1583 A       549 A       534 A
 14.00 keV    3.260E-01  3.332E-03    1681 A       563 A       552 A
 15.00 keV    3.359E-01  3.190E-03    1776 A       575 A       570 A
 16.00 keV    3.451E-01  3.062E-03    1869 A       587 A       586 A
 17.00 keV    3.537E-01  2.945E-03    1961 A       598 A       602 A
 18.00 keV    3.618E-01  2.838E-03    2052 A       608 A       617 A
 20.00 keV    3.766E-01  2.648E-03    2229 A       628 A       645 A
 22.50 keV    3.925E-01  2.448E-03    2444 A       649 A       678 A
 25.00 keV    4.062E-01  2.279E-03    2653 A       668 A       708 A
 27.50 keV    4.178E-01  2.135E-03    2858 A       685 A       735 A
 30.00 keV    4.276E-01  2.010E-03    3059 A       701 A       761 A
 32.50 keV    4.360E-01  1.900E-03    3257 A       716 A       786 A
```

| | | | | | |
|---|---|---|---|---|---|
| 35.00 keV | 4.430E−01 | 1.803E−03 | 3453 A | 729 A | 809 A |
| 37.50 keV | 4.489E−01 | 1.717E−03 | 3647 A | 742 A | 831 A |
| 40.00 keV | 4.538E−01 | 1.639E−03 | 3839 A | 754 A | 852 A |
| 45.00 keV | 4.612E−01 | 1.505E−03 | 4220 A | 777 A | 893 A |
| 50.00 keV | 4.658E−01 | 1.394E−03 | 4599 A | 798 A | 931 A |

| Multiply Stopping by | for Stopping Units |
|---|---|
| 2.7019E+01 | eV / Angstrom |
| 2.7019E+02 | keV / micron |
| 2.7019E+02 | MeV / mm |
| 1.0000E+00 | keV / (ug/cm2) |
| 1.0000E+00 | MeV / (mg/cm2) |
| 1.0000E+03 | keV / (mg/cm2) |
| 4.4804E+01 | eV / (1E15 atoms/cm2) |
| 2.8899E+01 | L.S.S. reduced units |